Accepted Manuscript

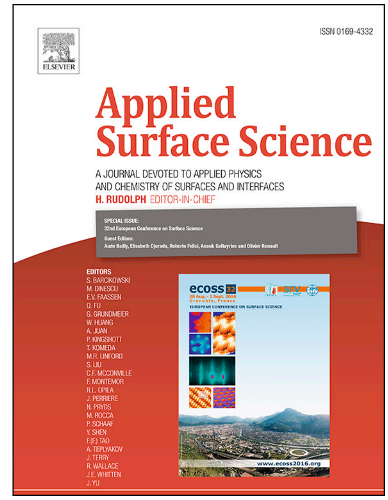


Full Length Article

# A Simple Method for Fabrication of Antifuse WORM Memories

J.A. Ávila-Niño, M. Reyes-Reyes, O. Nú ñez-Olvera, R. López-Sandoval

PII: S0169-4332(18)31433-8
DOI: https://doi.org/10.1016/j.apsusc.2018.05.126
Reference: APSUSC 39402

To appear in: *Applied Surface Science*

Received Date: 13 February 2018
Revised Date: 24 April 2018
Accepted Date: 17 May 2018

Please cite this article as: J.A. Ávila-Niño, M. Reyes-Reyes, O. Nú ñez-Olvera, R. López-Sandoval, A Simple Method for Fabrication of Antifuse WORM Memories, *Applied Surface Science* (2018), doi: https://doi.org/10.1016/j.apsusc.2018.05.126

# A Simple Method for Fabrication of Antifuse WORM Memories

J. A. Ávila-Niño[1,2,3], M. Reyes-Reyes[2], O. Núñez-Olvera[2] and R. López-Sandoval[1]*

[1] Advanced Materials Department, IPICYT, Camino a la Presa San José 2055, Col. Lomas 4a sección, San Luis Potosí 78216, Mexico.
[2] Instituto de Investigación en Comunicación Óptica, Universidad Autónoma de San Luis Potosí, Álvaro Obregón 64, San Luis Potosí 78000, Mexico.
[3] CONACYT - Centro de Investigación y Desarrollo en Electroquímica, Parque Tecnológico Querétaro s/n Sanfandila, Pedro Escobedo, Querétaro, 76703, México

## Abstract

A write-only-read-many (WORM) memory device was obtained by irradiating, with a commercial ultraviolet-ozone (UVO) lamp, the aluminium bottom electrode in an Al/$AlO_x$-UVO/Al configuration. The formation of conductive paths due Joule heating is observed when a positive or negative bias voltage is applied to the device, occurring a permanent transition from high (OFF) to low (ON) resistance state. After OFF to ON transitions, physical deformations were observed on the top of the devices, which were analyzed using morphological studies of the top electrode. To eliminate these physical deformations, the UVO treatment on the aluminium bottom electrode was replaced by the deposition of a thin polyvinyl alcohol (PVA) film (10 nm). These Al/$AlO_x$-native/PVA/Al WORM memories presented similar I-V behaviours and the same threshold voltages to those Al/$AlO_x$-UVO/Al devices, but with higher ON/OFF ratios. Analysis of the I-V curves confirms that the same physical phenomena, such as the formation of filamentary paths, are occurring for both types of devices.

## Introduction

Resistive memory devices consist generally in an active layer embedded between two metallic electrodes, which are able to change between a high resistance state (OFF) and low resistance state (ON). In the case of a permant change from OFF and ON, these memory devices are named write once read many times (WORM) memories, whereas when these memory devices can change several times between the OFF and ON they named rewritable memories. One of the main advantages of resistive memories, in comparison with the most common memories used in electronic components, is that they are nonvolatile, i.e. these retain information even if the power is turned off [1]. In particular, WORM memories have potential applications in ultra-low cost digital storage [2] and other permanent digital storage applications for video, images, electronic voting and non-editable database [3,4].

Nonvolatile memory behaviour has been observed for different organic and inorganic [5] composites used as active layers. WORM memories have been reported for metal/dielectric polymer/metal devices generally with polymer thickness < 100 nm [6]. It has been considered for several groups that the presence of an oxide film is the responsible for obtaining resistive switching in WORM memories [3,7,8]. Among the inorganic materials showing rewritable or WORM characteristics are several oxide films such as $TiO_2$ [9] and $Al_2O_3$ [10]. These oxides are deposited by different methods that are expensive and, in some cases, can involve temperature, like sputtering [11] and atomic layer deposition [12]. Sometimes, it is only necessary a thin oxide film, created by an oxidation of the surface of electrodes or at the interface between two thin films, for their applications in devices. For these reasons, several electrode-engineering methods like oxygen plasma exposition [13], ultraviolet-ozone (UVO) lamp [14], natural exposition to the atmosphere [15,16] and ozone irradiation [17] have been used in order to obtain a thin oxide film. Using some of these surface modification techniques allow to compare, for example, the differences in the physicochemical properties due to the oxidation of an aluminium thin film by oxygen and ozone [17, 18]; it is found that the film irradiated with $O_3$ showed an increment of the insulating properties related with the increase of the barrier width [19]. Additionally, it has been reported that the irradiation of aluminium films with an UVO lamp improves their insulating properties and diminishes the leakage current in organic thin film transistors [14]. The improvement of the insulating property by ozone irradiation has been observed using other insulator materials like $Ta_2O_5$ [20].

In general, the switching mechanism of rewritable memory devices based on aluminium oxides ($AlO_x$) can be explained by the formation and destruction of filaments in the aluminium oxide film [4,21]. In the case of WORM memories, the conductive filaments in the oxide film can only be created and not destroyed [3, 8, 22, 23]. Recently, it has been reported Al/Al-rich $AlO_xN_y$/Si WORM memory in devices [8] and, for these devices, it has been argued that oxygen vacancies could generate filaments that form conductive paths, which cannot be destroyed unless a high temperature would be applied. A similar explanation was reported by Liu et al. [3], who obtained WORM memory devices by irradiating $O_2$ plasma onto a film of indium gallium zinc oxide (IGZO) in Al/IGZO/Al devices. They proposed an irreversible formation of a conductive of oxygen vacancies filament between both electrodes. Additionally, WORM characteristics for Pt/$Al_2O_3$/ITO devices have been reported, where the aluminium oxide were growth by molecular beam epitaxy [4].

In a previous report we found that irradiating for one minute the aluminium bottom electrode with an UVO lamp of Al/$AlO_x$-UVO/poly(3,4-ethylenedioxythiophene): polystyrene sulfonate (PEDOT:PSS) + carbon nanotube/Al rewritable memory device, their memory characteristics were improved due to physicochemical changes occurring on its surface. On the other hand, if the irradiation time is increased up to 30 minutes, the memory characteristics practically disappear due to an augmentation of $AlO_x$ layer from 2.8 nm, native $AlO_x$ layer, to 4.0 nm as a function of UVO treatment time, i.e. the formation of a very insulating oxide film on the bottom electrode [24]. In the present work, we show that a permanent storage of information can be fabricated by irradiating the aluminium bottom electrode using an UVO lamp for 30 minutes to create a 4.0 nm insulating $AlO_x$ layer in Al/$AlO_x$-UVO/Al devices. These Al/$AlO_x$-UVO/Al devices presented physical deformations on the top of them during the voltage sweep. These deformations are related with the creation of conductive paths or aluminium conductive filaments, and are indication of the permanent change of the devices from OFF to ON state. If the aluminium bottom electrode is not UVO irradiated, i.e. only has its native aluminium oxide layer, the Al/$AlO_x$-

native/Al devices do not show the physical deformation nor memory characteristics. Additionally, and for contrast, we have fabricated WORM memories by using organic insulator films of polyvinyl alcohol (PVA) with a thickness of ~ 10 nm between two aluminium electrodes. In these devices, the bottom electrode was not UVO irradiated. PVA has been previously used in two terminal resistive memory devices as the active layer or as the supporting layer due to its advantages such as water solubility; it is easily processed, present strong thermal and chemical resistance as well as excellent electrical properties [25-27]. PVA films in combination with carbon nanotubes [25] or reduced graphene oxide decorated with Au particles [26] have shown electrical switching. Additionally, it has been shown that rewritable memory devices based in graphene oxide nanosheets embedded in PVA matrix present better performance and a higher ON/OFF ratio compared with the devices not containing graphene oxide [27]. Our Al/$AlO_x$-native/PVA/Al devices show WORM memory behaviour, although do not present visible physical deformation on the top electrodes, suggesting the formation of conductive aluminium filaments inside the PVA film due to electrical electroforming during a voltage sweep. Our results represent a facile and economic way to fabricate stable WORM memory devices.

## Experimental

Before the deposition of the Al bottom electrode, the 1 $in^2$ Dow Corning glass substrates were cleaned by washing them in acetone, methanol and isopropanol in ultrasonic baths for 20 min and then dried for 40 min. Immediately, after evaporation of the solvents, the substrates were maintained in a UV-ozone ambient for 25 min. After that, a 90 nm Al bottom electrode was deposited by thermal evaporation at $10^{-6}$ Torr and patterned using a shadow mask. For Al/$AlO_x$-UVO/Al devices, the bottom electrode was irradiated by 30 minutes in an UV-Ozone environment using a commercial lamp in order to increase the thickness of the native $AlO_x$ insulating layer. For the fabrication of Al/$AlO_x$-native/PVA/Al devices, a composite of PVA (Sigma-Aldrich, Mw =9000-10000) and deionized water (1 wt%) was magnetically stirred overnight and spin coated at 6000 rpm by 40 seconds. Then, the PVA film was dried for 15 min at 100°C in an oven. The PVA and aluminum film thicknesses were measured using a Tencor Alpha-Step 500 surface profiler and were approximately 10 nm and 90 nm, respectively. Finally, a 90 nm thermally evaporated top electrode was deposited on Al/$AlO_x$–UVO, or on the polymeric composite PVA layer, and patterned using a shadow masks. Two different active areas, corresponding to the overlap of bottom and top electrodes, were used: 6 $mm^2$ and 0.25 $mm^2$ for both types of memories.

Current-voltage measurements were performed using a programmable Keithley 236 source meter at room conditions. In all the current-voltage measurements of the memory devices, the bias voltage is applied to the top electrode with the bottom electrode grounded. The morphological characterizations of the rewritable memory devices were performed using a Quanta 250 scanning electron microscope, operated at 20 kV, and a Jeol JSPM-5200 atomic force microscope in contact mode. AFM micrographs were processed using WSXM software [28].

## Results

The Al/$AlO_x$-UVO/Al devices were I-V characterized using voltage sweeps from 0 to 4 V, 4 to – 4 V and -4 to 0 V (Fig. 1a) or from 0 to -4 V, -4 to 4 V and 4 to 0 V (Fig. 1b). For both cases, the pristine memory devices start in the OFF state (~$10^{-3}$ A at ±1 V) until a threshold voltage is reached, then the current increases switching permanently the device to the ON (~$10^{-1}$ A for both polarities) state. The devices present symmetrical switching behaviour during the electroformation of the pristine devices, showing threshold voltages of ~ 2 V for positive bias (Fig. 1a) and ~ -2 V for negative bias (Fig. 1b). Using a second voltage sweep, it can be corroborated that the memory devices present WORM characteristics. The fabricated memory devices have an ON/OFF ratio between 1.5 and 2 orders of magnitude at a read voltage of 1 V. On the other hand, Al/$AlO_x$-native/Al devices, i.e. with no UVO exposition on the bottom electrode, showed an ohmic behaviour, before electrical current reaches the compliance current of the Keithley multimeter (Fig. S1).

It has been reported in ITO/$Al_2O_3$/Pt WORM devices that when the threshold voltage is reached, the oxygen vacancies act as electron traps and these vacancies migrate due to the electrical field applied across the device forming a conductive filament in the oxide film [4]. Additionally, in the ITO/$Al_2O_3$/Pt WORM devices, the pristine memory devices start in the high conductive ON state. However, our Al/$AlO_x$-UVO/Al devices start in the high resistive OFF state, thus, the physical phenomenon responsible of the resistive switching is not the movement of oxygen vacancies, but the creation of metallic filament paths due to the high electrical field during the electroforming process. These metallic pathways across the aluminium oxide film are observed as physical deformation on the top electrode. SEM micrographs showed that paths are created along the most of the overlapping area of the two electrodes (Fig. 2a); the image amplification shows aluminium pathways that have circular craters (Fig. 2b). 2D (Fig. 3a) and 3D (Fig. 3b) AFM micrographs of the top electrode of Al/$AlO_x$-UVO/Al devices show the morphology of these deformations. The profile of the line drawn in the Fig. 3a, using WSXM software, shows that the craters have the depth of approximately two aluminium electrodes (Fig. 3c); the aluminium oxide layer is very thin. Then, aluminium was removed from some regions of the active area creating conductive pathways in the contour of the craters with height of ~ 400 nm (with height of ~ 4 aluminium layers). The voltage stress applied to the device induced the melting of the aluminium films forming an overlapping of the two aluminium layers. The creation of these conductive paths occurs when a threshold voltage is reached, not depends of the polarity and is irreversible. These paths are created by the dielectric breakdown of the insulating layer due to the higher electric field in the $AlO_x$ film. This dielectric breakdown can be qualitatively understood considering the memory device as a parallel plate MIM capacitor. The dielectric strength of alumina, $Al_2O_3$, is ~13.4 MV/m and has an electrical constant $\varepsilon_{\text{alumina}} \approx 10$, whereas the strength of the electric field $E$ in the active layer for a parallel plate MIM capacitor with a alumina layer with thickness $d \approx 4$ nm at 2V is $E = 2V/(d\varepsilon_{alumina}) \approx 50$MV/m. The process of dielectric breakdown of an oxide dielectric, has been proposed that is performed in three steps: (a) an electron percolation path is established, which is carried out through the dielectric grain boundaries, in our case the aluminum oxide; (b) as the current flow through these percolative paths increases, the Joule heating process takes place and results in an increase in the area of the percolative paths. Finally, (c) the Joule heating is so intense that the materials in contact, the aluminum oxide and the electrodes of aluminum, melt and atoms of these materials can be introduced into the percolative paths [29]. This mechanism explains the electrodes melting observed in the SEM images (Fig. 2) and in the AFM micrographs (Fig. 3). This type of organic memories, based on the dielectric breakdown of the active layer, is generally called antifuse memories. On the other hand, Al/$AlO_x$-native/Al devices, without UVO irradiation on the bottom electrode, show neither memory behaviour nor physical deformation when a voltage stress was applied at the device. This is because the native aluminium oxide layer, consisting of hydroxide and aluminium oxide, is very thin, approximately 2.8 nm, [24] in such a way that the electrons can easily tunnel through it.

A method to eliminate the visible physical deformation on the top electrode was using an organic very thin film (~10 nm) of a water-soluble polymer (PVA) embedded between two aluminium electrodes, without UVO treatment on the bottom electrode. The increase of the insulator layer thickness up to 12.8 nm (10 nm of PVA + 2.8 nm of native oxide layer) as well as the increase in the dielectric strength of the active layer decrease the strength of the electric field $E$ inside of the active layer; the dielectric strength of PVA is approximately ~50 MV/m whereas its dielectric constant is $\varepsilon_{PVA} \approx 2$ [30]. Therefore, the dielectric breakdown of the active layer is softer (Fig. S2). These Al/$AlO_x$-native/PVA/Al devices showed WORM behavior and this fabrication method is an alternative to obtain very cheap WORM memories with good electrical characteristics. In these devices (Figs. 4a and 4b), a higher ON/OFF ratio (~4 orders of magnitude) could be attributed to a higher thickness of the active layer, PVA film (~10 nm) and the native aluminium oxide (~2.8 nm) compared with the thickness of the aluminium oxide layer due to UVO treatment (~ 4 nm) [24]. Additionally, it can observe from these figures that the electrical current levels in the OFF state of Al/$AlO_x$-native/PVA/Al devices are considerable lower, around four orders of magnitude at a read voltage of -1 V, in comparison with the Al/$AlO_x$-UVO/Al devices (Fig. 2), implying that the PVA layer reduces the magnitude of the electrical current passing through the device. Note that the tunnelling current depends on the energy barrier as well as the width of this barrier [31]. Thus, the differences in current levels in the OFF state in both kind of devices are related to differences in energy gaps of the insulating layers ($AlO_x$ has a bandgap of 8.8 eV in its crystalline form [31] and between 5-7.1 eV for its amorphous form [32] while PVA has a bandgap of 5.4 eV [33]) as well as the thickness of the insulating layers. On the other hand, the differences in the current levels in the ON state between both devices are not so different (~ 1 order of magnitude). In the Al/$AlO_x$-native/PVA/Al memory devices, we consider that conductive filaments have being created through the polymer layer, although no physical deformations were observed on the top electrode. i.e. the presence of the PVA layer between both aluminium electrodes softens the dielectrical breakdown and minimizes heating Joule effects (Fig. S2). Thus, the use of PVA as insulator and dielectrical layer hinders the current flow through the device; the Joule heating is not so intense and no melt of aluminium electrodes is achieved. Therefore, the creation of the conductive filaments in the PVA layer is due to the migration of atoms from the electrodes in metal-insulator-metal devices; this has been a recurrent explanation in this type of WORM memories in different systems and using different metallic electrodes [34]. These effects have been observed in a previous report, when we fabricated Al/polymethyl methacrylate (PMMA)/Al and Al/ polystyrene (PS)/Al devices [23] and where introduction of aluminium particles, due to an applied bias voltage, could be observed in the polymeric films after top electrode delamination. Other materials with similar electrical properties, such as PMMA with energy band gap of 5.6 eV [35] and dielectrical constant of 3.6 [36] could be also used as softener layer. However, there are other physical and chemical properties that should be considered. One of the advantages of the use of PVA is its great solubility in water, which is not flammable and a harmless solvent, while PMMA is highly soluble in organic solvents such as chlorobenzene or chloroform, which are flammable and exhibit degrees of toxicity from low to moderate. Other important parameter is the wettability of the polymer layer on the metal electrode, where the chemical composition and thickness of the oxide layer affect the wettability and adhesion of polymers [24,37]. Even more, it is known that the outermost surface layer of oxide films is covered with a layer of hydroxyl groups and the nature of these surface hydroxyl groups determines the physicochemical properties of the surface of the films [24,37]. PVA present well wettability and adhesion properties on the aluminium electrode and, for this reason, we have a pinhole free polymeric layer with a thickness ≈10 nm whereas that is not possible in the case of using PMMA as an active layer [23].

The stability of both types of memory devices was also measured. First, the OFF state was read by the application of pulses of -1 V for $10^3$ times. After that, a negative bias is applied (0 to -4 V) to switch the device to the ON state and then, the ON state was read for $10^3$ times by the application of -1 V pulse. Al/$AlO_x$-UVO/Al (Fig. 5a) as well as Al/$AlO_x$ native/PVA/Al (Fig. 5b) showed good stability. In order to elucidate the charge transport mechanism in both memory states, ON and OFF, as well as to understand the electroformation process in both kind of memory devices, log (V) vs log (I) curves, for

$Al/AlO_x$-UVO/Al (Fig. 6a) and $Al/AlO_x$-native/PVA/Al (Fig. 6b), have been analyzed using conduction models. From this analysis, we obtain that ON state for both type of memory devices can be described using an ohmic model; the slope is m~1 for both $Al/AlO_x$-UVO/Al and Al/AlOx-native/PVA/Al devices indicating metallic filaments have been created when a threshold voltage is reached. Their respective OFF states, on the other hand, are well described by the ohmic model for low voltages ($\leq$ 0.4 V) and by the space-charge-limited-current (SCLC) model for higher voltages ($\geq$ 0.4 V), which is in good agreement with WORM memories reported in the literature [38]. The slope for the $Al/AlO_x$-UVO/Al device for voltages between 0.45 and 1.8 V is m~2.2 and the slope for the $Al/AlO_x$-native/PVA/Al device is m~2.5 for the same voltage range. Slopes higher than m~2 ($I \sim V^2$) suggest that the SCLC model is dominant in the OFF state as $I \sim V^{m+1}$ with m $\geq$1 [39]. The slopes of the log (V) vs log (I) curves for OFF and ON states are very similar in both types of devices, then, it is expected that the same physicochemical phenomena are occurring if Al-UVO treated layer or PVA film are used as the active area. The differences in the electrical currents for ON and OFF states of the devices and in ON/OFF ratios can be related to differences in the electrical properties between PVA and aluminium oxide, as well as the higher thickness of PVA film compared with the aluminium oxide film. In addition, the transition from OFF to ON states is more abrupt in the PVA memories due the same reasons. Nevertheless, both devices present basically the same behaviour for ON and OFF states, which suggests that metallic filaments were created through PVA films although no physical deformations are observed on the top electrode. Furthermore, $Al/AlO_x$-UVO/Al devices as well as $Al/AlO_x$-native/PVA/Al could be scaled using shadow masks. I-V curves of both type devices with an active area of 0.25 $mm^2$ (~500 μm x 500 μm) show WORM behaviour for negative and positive sweeps (Figs. S3 and S4). It is important to note that both type of devices show symmetrical I-V characteristics. SEM micrograph of the top electrode of $Al/AlO_x$-UVO/Al devices shows similar physical deformation and these deformations are confined in the overlapping area after several voltage sweeps were applied (Fig. S5). These results show that these WORM devices can be miniaturized increasing their data storage.

## Conclusions

A simple way to obtain very simple WORM memories was presented, which consists of an aluminium bottom electrode irradiated with a commercial UVO lamp by 30 minutes and an aluminium top electrode. These Al/$AlO_x$-UVO/Al devices present an ON/OFF ratio of ~ $10^2$ and the ON and OFF states retain the information for at least $10^3$ times. When a voltage sweep was applied to the pristine device, physical deformation on the top electrode were observed implying that physical pathways, due to Joule heating, were created forming irreversible high conductive pathways. Additionally, Al/$AlO_x$-native/PVA (~10 nm)/Al devices were fabricated, which show WORM memory behaviour but without any physical deformation on the top electrode, which implies that PVA layer acts as a softener layer reducing the electrical current passing through the device and, therefore, minimizing the Joule heating effects. These Al/$AlO_x$-native/PVA/Al devices present similar retention characteristics than the Al/$AlO_x$-UVO/Al devices and higher ON/OFF ratios ($10^4$). The I-V characteristics of both types of devices were analyzed using various conduction models and these showed similar behaviour, their states OFF can be described by ohmic model for low voltage (< 0.4 V) and SCLC mode for voltage between 0.45 and 2.2 V, whereas their ON state is described by ohmic model. This corroborates that the same physical phenomena are occurring in the electroforming process for both devices: the creation of conductive pathways when the device is under voltage stress. The devices could be scaled down ~24 times presenting basically the same behaviour.

## Acknowledgments

The authors acknowledge M. Sc. Beatriz A. Rivera, M. Sc. Ana I. Peña, Dr. Gladis Labrada and Dr. Hector G. Silva-Pereyra for technical assistance as well as to LINAN at IPICyT for providing access to its facilities. This work was supported by CONACYT through grant No. CB-2015-01-256484 (R.L.S) J.A.A.N. thanks to the Fondo Sectorial-CONACYT-SENER-Hidrocarburos for a posdoctoral grant (2137).

**Figures**

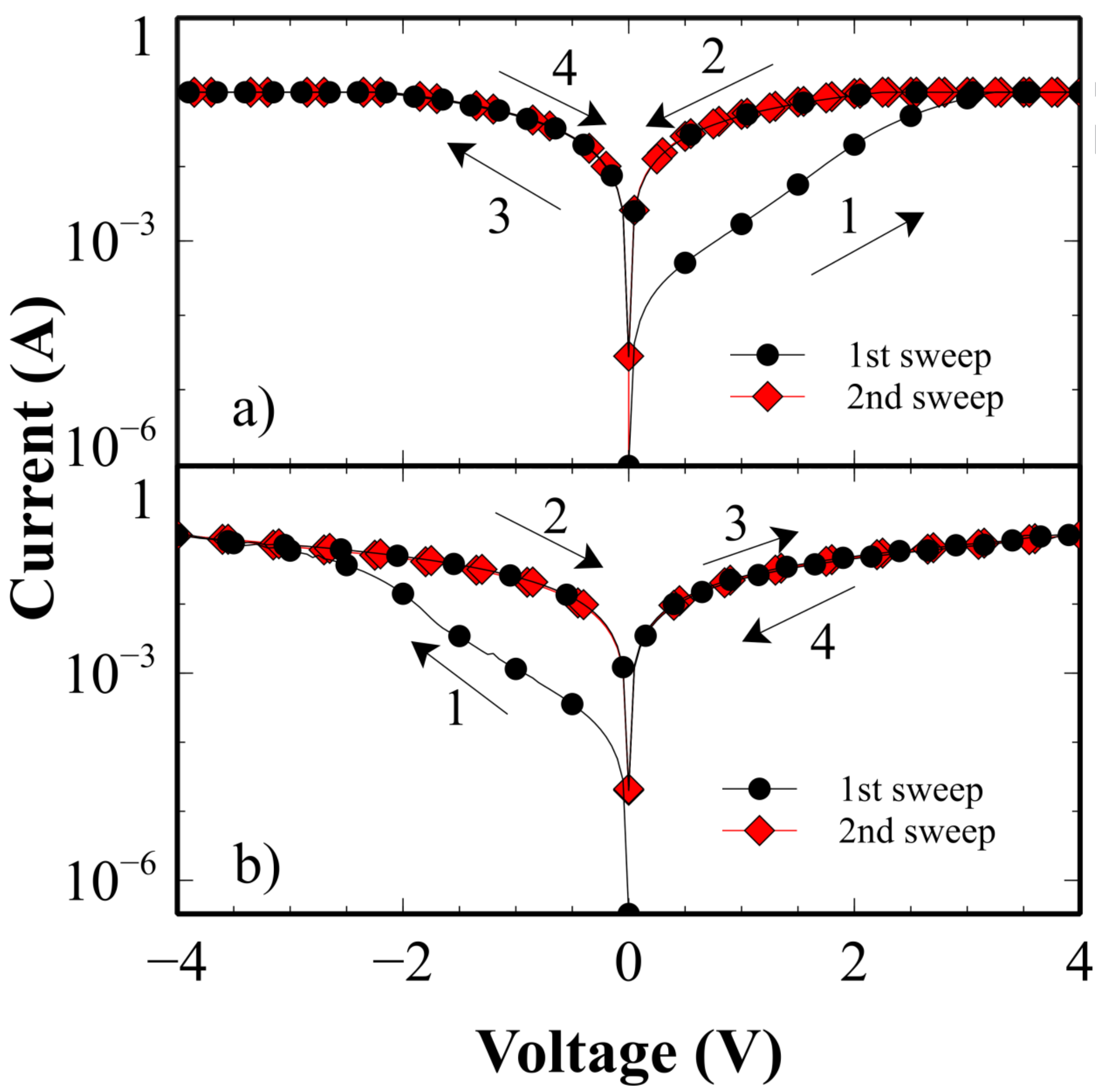


Figure 1. I-V characteristics of: a) of Al/$AlO_x$-UVO/Al device with voltage sweep from 0 to 4 V, 4 to -4 V and -4 to 0 V and b) of Al/$AlO_x$-UVO/Al device with voltage sweep from 0 to -4 V, -4 to 4 V and 4 to 0 V.

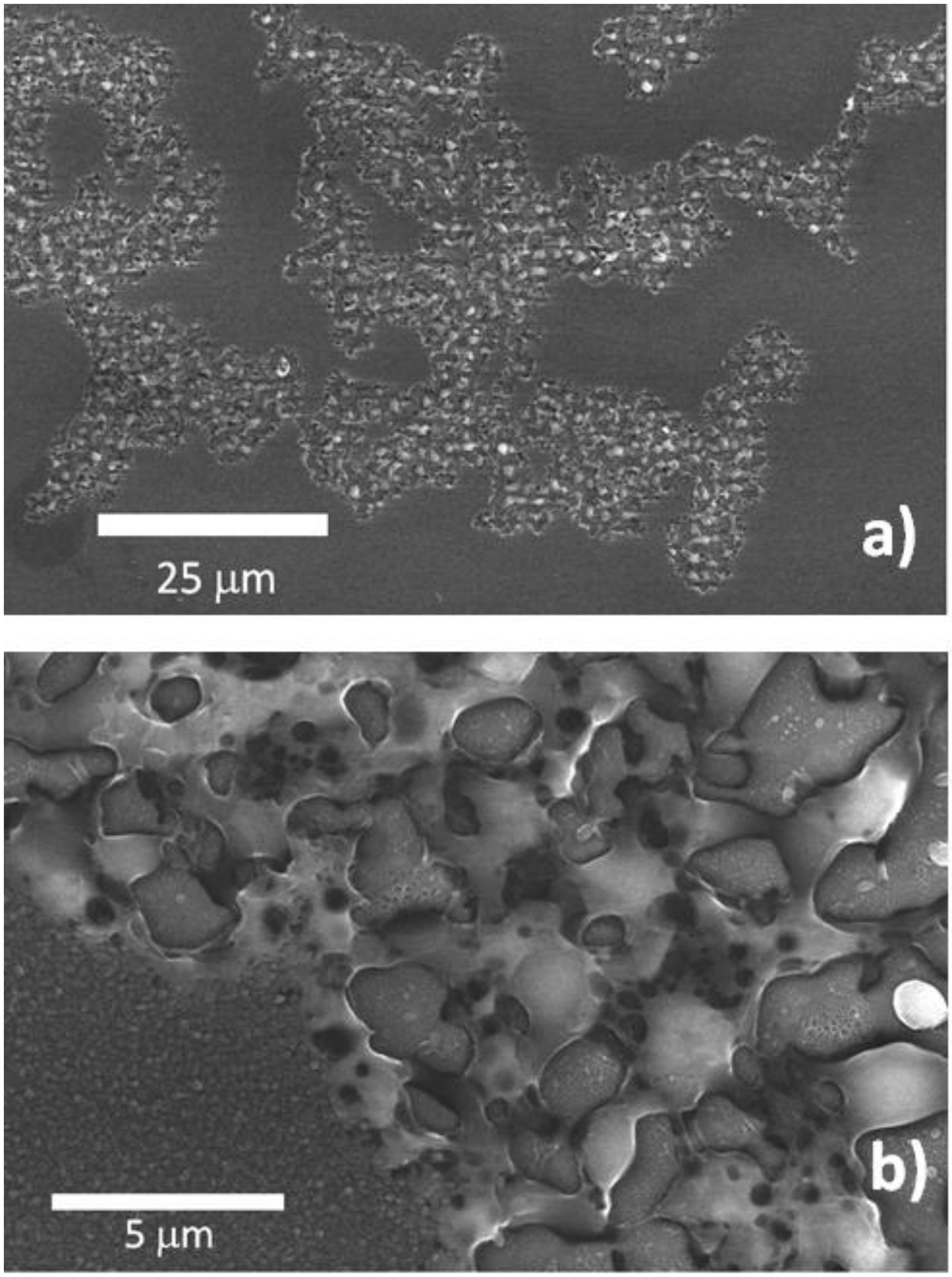


Figure 2. SEM micrographs at two different scales of the top electrode of the Al/$AlO_x$-UVO/Al device after several voltage sweeps between -4 and 4 V.

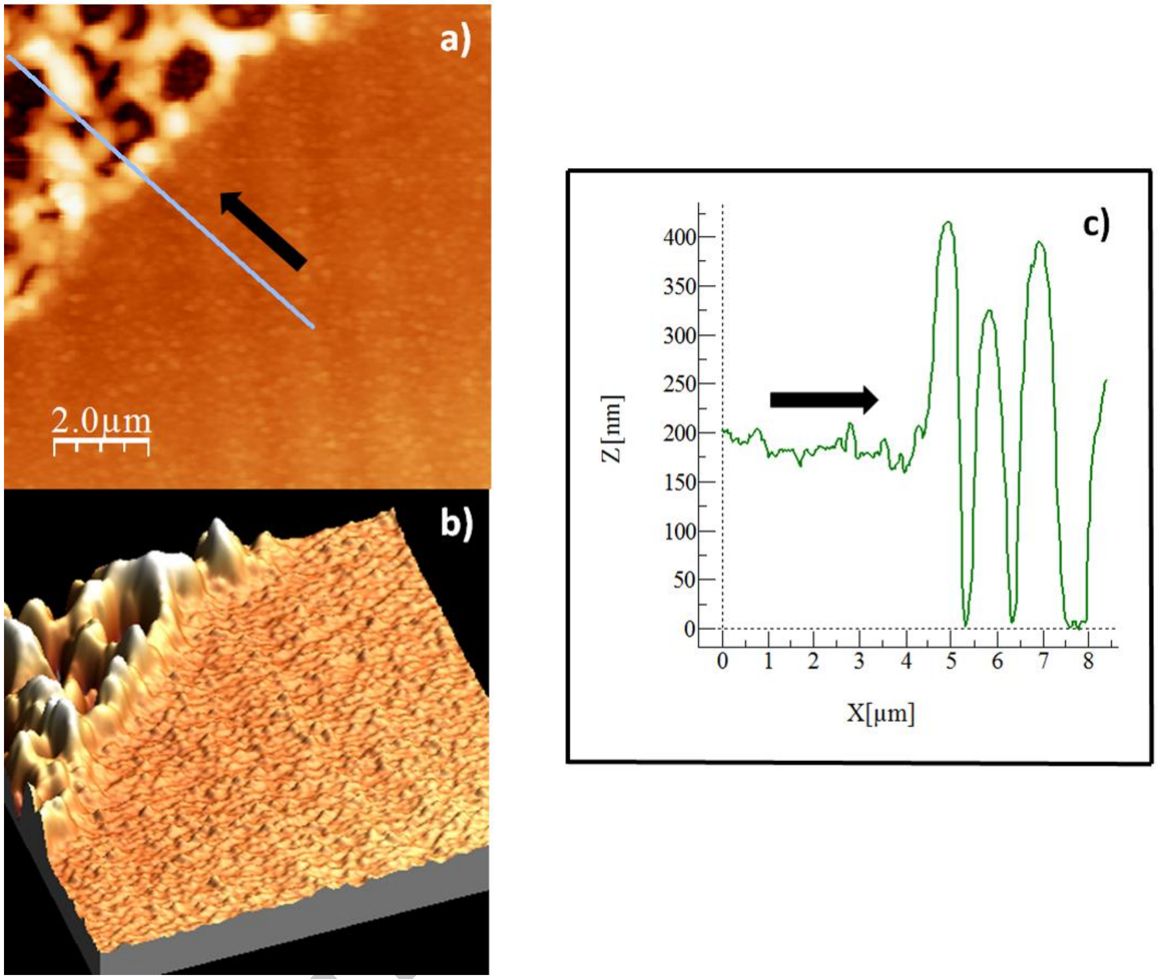


Figure 3. a) 2D-AFM micrograph of the top electrode of Al/$AlO_x$-UVO/Al device after the application of several voltage sweeps between -4 and 4 V. b) 3D-AFM micrograph in the same region than a), and c) profile obtained following the line showed in a).

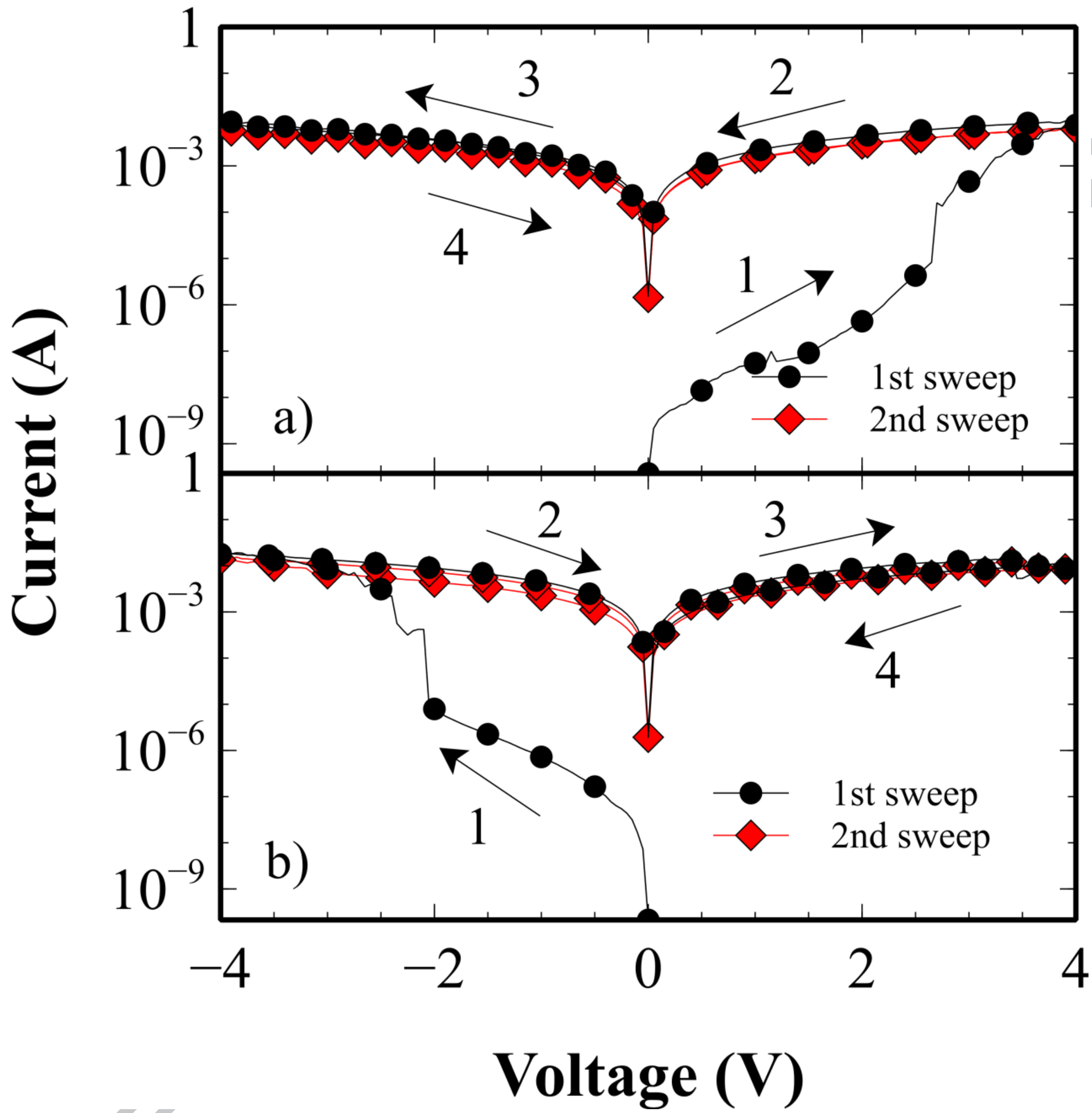


Figure 4. I-V characteristics of a) of Al/$AlO_x$-native/PVA/Al device with voltage sweeps from 0 to 4 V, 4 to -4 V and -4 to 0 V and b) Al/$AlO_x$-native/PVA/Al device with voltage sweep from 0 to -4 V, -4 to 4 V and 4 to 0 V.

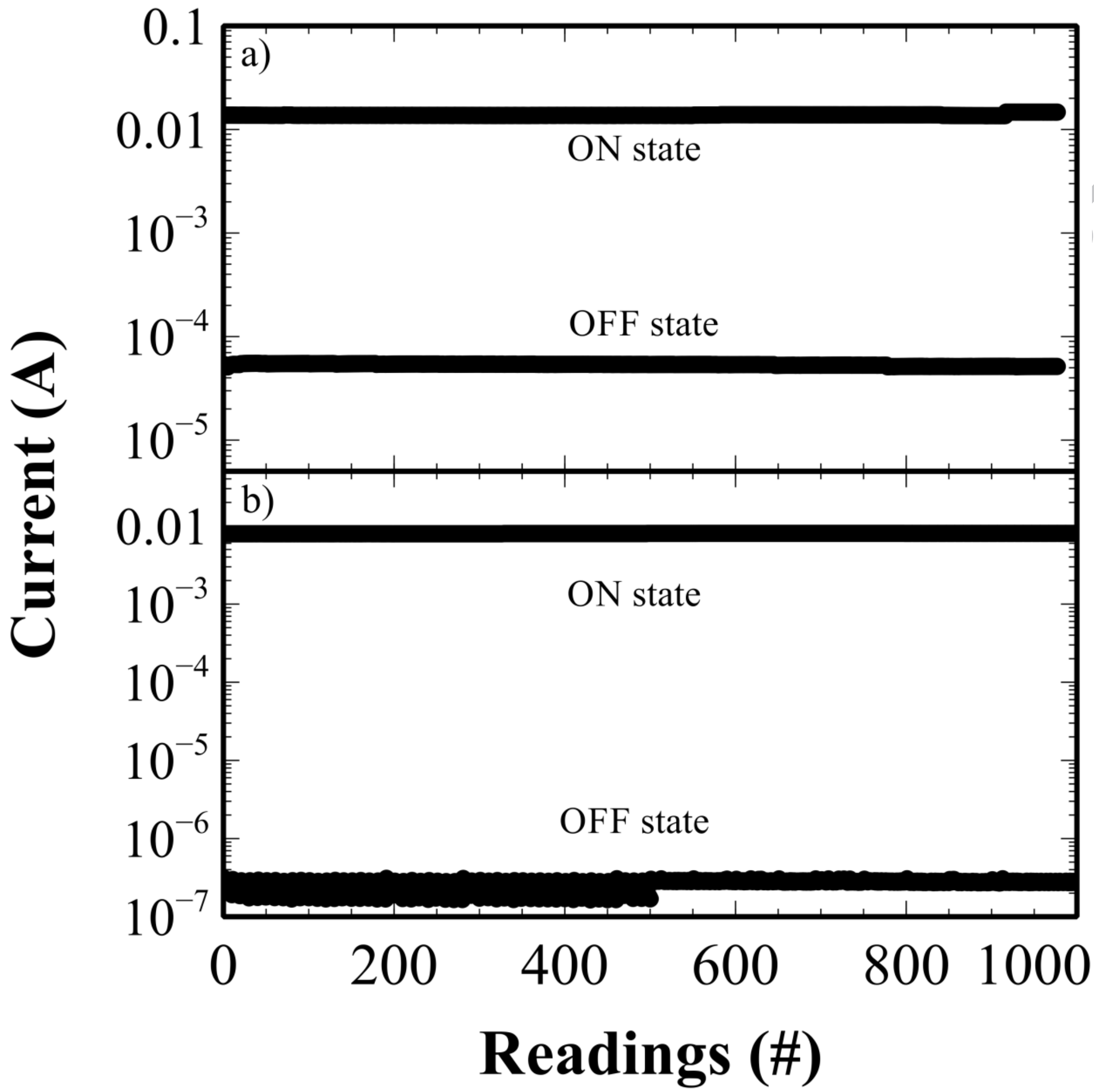


Figure 5. Number of readings of the ON and OFF states at -1 V of: a) Al/$AlO_x$-UVO/Al and b) Al/$AlO_x$-native/ PVA/Al devices.

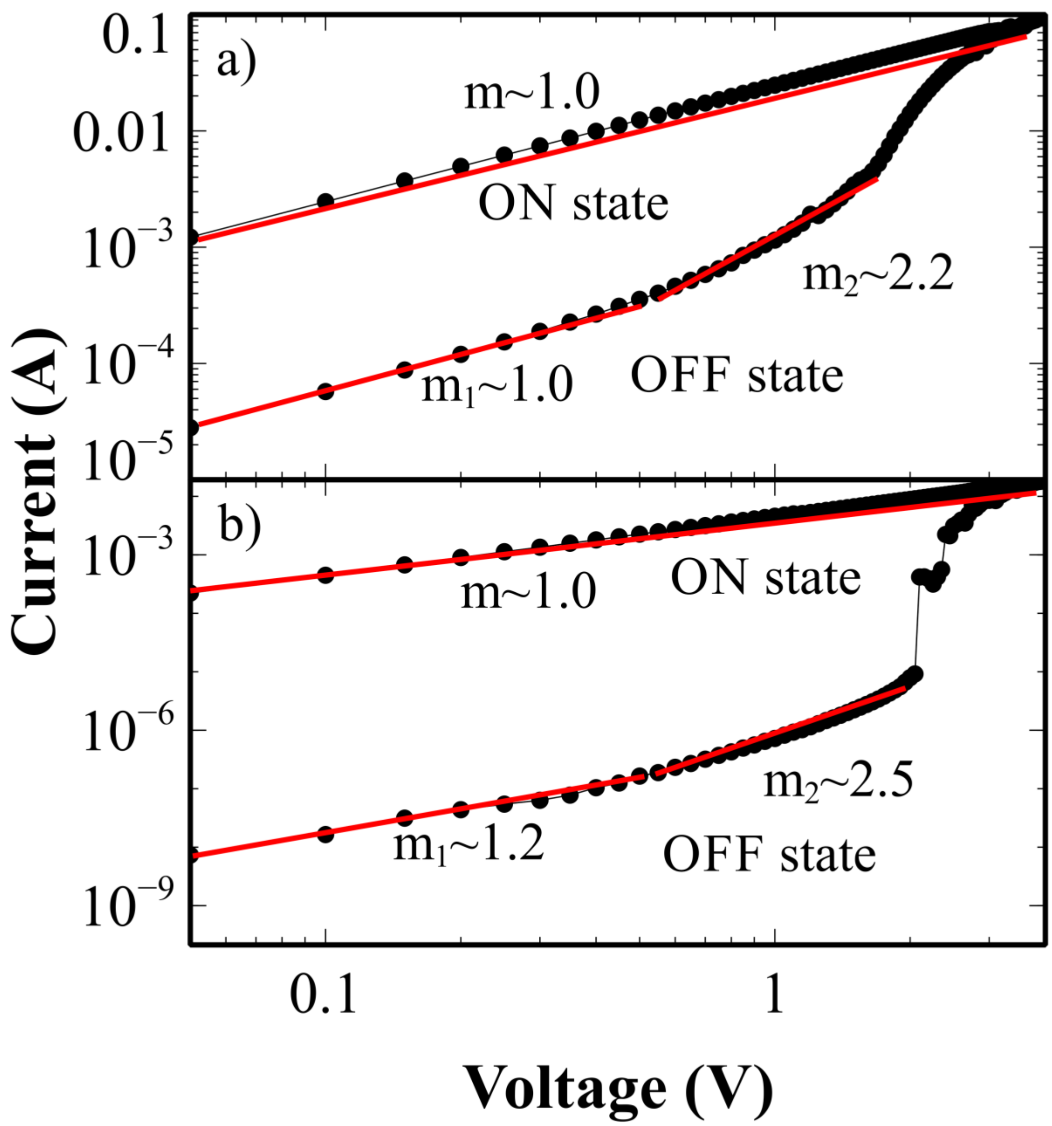


Figure 6. Log (V) vs Log (I) curves for: a) Al/$AlO_x$-UVO/Al devices and b) Al/$AlO_x$-native/PVA/Al devices.

**References**


[1] Q.D. Ling, D.J. Liaw, C. Zhu, D.S.H, Chan, E.T. Kang and K.G. Neoh, Polymer electronic memories: Materials, devices and mechanisms, Progress in Polymer Science 33 (2008) 917–978

[2] S. Möller, C. Perlov, W. Jackson, C. Taussig, S. R. Forrest, A polymer/semiconductor write-once read-many-times memory, Nature 426 (2003) 166-169.

[3] P. Liu, T. P. Chen , X. D. Li, Z. Liu, J. I. Wong, Y. Liu, K. C. Leong, Realization of write-once-read-many-times memory device with O2 plasma-treated indium gallium zinc oxide thin film, Appl. Phys. Lett. 104 (2014) 033505

[4] S.Wu, X. Chen, L. Ren, W. Hu, F. Yu,1 K. Yang, M. Yang, Y. Wang, M. Meng, W. Zhou, D. Bao, S. Li, Write-once-read-many-times characteristics of Pt/Al2O3/ITO memory devices, J. Appl. Phys. 116 (2014) 074515

[5] A. Chen, A review of emerging non-volatile memory (NVM) technologies and applications, Solid-State Electronics 125 (2016) 25–38

[6] J.H. Jung, W.Y. Kim, D.K. Kim,1 J.H. Kwon, H. C. Lee, J.H. Bae, Observation of Irreversible Current Path in Polymer Dielectric using Conductive Atomic Force Microscope, Electron. Mater. Lett. 11 (2015), 246-251

[7] A. Sawa, Resistive switching in transition metal oxides, Mater. Today 11 (2008) 28-36

[8] W. Zhu, J. Li, L. Zhang, X.C. Hu, A reversible bipolar WORM device based on AlOxNy thin film with Al nano phase embedded, Solid-State Electronics 129 (2017) 134–137

[9] J. J. Yang, F. Miao, M. D. Pickett, D. A. A. Ohlberg, D. R. Stewart, C. N. Lau, R. S. Williams, The mechanism of electroforming of metal oxide memristive switches, Nanotechnology 20 (2009) 215201

[10] S. Karthäuser, B. Lüssem, M. Weides, Resistive switching of rose bengal devices: A molecular effect? J. Appl. Phys. 100 (2006) 094504

[11] F. Verbakel, S. C. J. Meskers, and R. A. J. Janssen, H. L. Gomes, M. Cölle, M. Büchel, and D. M. de Leeuw, Appl. Phys. Lett. 91 (2007) 192103

[12] W. Lee, J. Jang, Y. Song, K. Cho, D. Yoo, Y. Kim, S. Chung, T. Lee, Attachable and flexible aluminum oxide resistive non-volatile memory arrays fabricated on tape as the substrate, Nanotechnology 28 (2017) 135201

[13] B. Cho, S. Song, Y. Ji, T. Lee, Electrical characterization of organic resistive memory with interfacial oxide layers formed by O2 plasma treatment, Appl. Phys. Lett. 97 (2010) 063305

[14] S. Gupta, S. Hannah, C.P. Watson, P. Šutta, R.H. Pedersen, N. Gadegaard, H. Gleskova, Ozone oxidation methods for aluminum oxide formation: Application to low-voltage organic transistors, Organ. Electron. 21 (2015) 132–137

[15] D.S. Jeong, B. Cheong, H. Kohlstedt, Pt/Ti/Al2O3/Al tunnel junctions exhibiting electroforming-free bipolar resistive switching behaviour, Solid-State Electronics 63 (2011) 1–4

[16] K.S. Yook, J.Y. Lee, S.H. Kim, J. Jang, Transparent organic bistable memory device with pure organic active material and Al/indium tin oxide electrode, Appl. Phys. Lett. 92 (2008) 223305

[17] A. Kuznetsova, I. Popova, V. Zhukov, and J. T. Yates, Jr., G. Zhou and J. C. Yang, X. Chen, J. Vac. Sci. Technol. A 19 (2001) 1971-1976.

[18] A. Kuznetsova, J. T. Yates, Jr., G. Zhou and J. C. Yang, X. Chen, Making a Superior Oxide Corrosion Passivation Layer on Aluminum Using Ozone, Langmuir 17 (2001) 2146-2152

[19] B. G. Park, J. Y. Bae, T. D. Lee, Growth characteristics of Al oxide formed by ozone in magnetic tunnel junctions, J. Appl. Phys. 91 (2002) 8789-8791

[20] B.K. Moon, C. Isobe, J. Aoyama, Insulating properties of tantalum pentoxide capacitor films obtained by annealing in dry ozone J. Appl. Phys. 85 (1999) 1731-1738,

[21] K. Park, J.S. Lee, Reliable resistive switching memory based on oxygen-vacancy-controlled bilayer structures, RSC Adv. 6 (2016) 21736

[22] S. Kim, Y.K. Choi, Resistive switching of aluminum oxide for flexible memory, Appl. Phys. Lett. 92 (2008) 223508

[23] J. A. Avila-Niño, A. O. Sustaita, M. Reyes-Reyes, R. López-Sandoval, Effect of the Thickness of Insulator Polymeric Films on the Memory Behavior: The Case of the Polymethylmethacrylate and the Polystyrene, J. Nanotechnology 2011 (2011) 702464

[24] I.A. Rosales-Gallegos, J.A. Avila-Niño, M. Reyes-Reyes, O. Núñez-Olvera, R. López-Sandoval, Effect of the oxidation of aluminium bottom electrode in a functionalized-carbon nanotube based organic rewritable memory device, Thin Solid Films 619 (2016) 10–16

[25] S. Chandrakishore, A. Pandurangan, Facile synthesis of carbon nanotubes and their use in the fabrication of resistive switching memory devices, RSC Advances 4 (2014) 9905;

[26] A. Midya, N. Gogurla, S. K. Ray, Flexible and transparent resistive switching devices using Au nanoparticles decorated reduced graphene oxide in polyvinyl alcohol matrix, Current Applied Physics 15 (2015) 706-710

[27] Y. Sun, J. Lu, C. Aib, D. Wen, Nonvolatile memory devices based on poly(vinyl alcohol) + graphene oxide hybrid composites, Phys. Chem. Chem. Phys. 18 (2016) 11341

[28] I. Horcas, R. Fernandez, J. Gomez-Rodriguez, J. Colchero, J. Gomez Herrero and A. M. Baro, WSXM: a software for scanning probe microscopy and a tool for nanotechnology, Rev. Sci. Instrum. 78 (2007) 013705.

[29] R. Ranjen, K. Pey, L. Tang, G. Groeseneken, L. Bera, S. Gendt, A comprehensive model for breakdown mechanism in $HfO_2$ high-gate stacks IEDM Conf. Proc. 2004, (2004) 725-728.

[30] N. Ning, X. Bai, D. Yang, L. Zhang, Y. Lu, T. Nishi and M. Tian, Dramatically improved dielectric properties of polymer composites by controlling the alignment of carbon nanotubes in matrix, RSC Adv. 4 (2014) 4543–4551

[31] J. Robertson, Band offsets of wide-band-gap oxides and implications for future electronic devices, J. Vac. Sci. Technol. B 18 (2000) 1785-1791.

[32] S. Toyoda, T. Shinohara, H. Kumigashira, M. Oshima, Y. Kato, Significant increase in conduction band discontinuity due to solid phase epitaxy of Al2O3 gate insulator films on GaN semiconductor, Appl. Phys. Lett. 191 (2012) 231607−231610.

[33] S. B. Aziz, Modifying poly(vinyl alcohol) (PVA) from insulator to small-bandgap polymer: a novel approach for organic solar cells and optoelectronic devices, J. Electron. Mater. 45 (2016) 736-745.

[34] V.C. Nguyen, P. S. Lee, Optically readout write once read many memory with single active organic layer Appl. Phys. Lett. 108 (2016) 033301

[35] D. I. Son, C. H. You, J. H. Jung, T. W. Kim, Carrier transport mechanisms of organic bistable devices fabricated utilizing colloidal ZnO quantum dot-polymethylmethacrylate polymer nanocomposites, Appl. Phys. Lett. 97 (2010) 013304.

[36] J. Brandrup, E.H. Immergut, E.A. Grulke, Polymer Handbook, 2nd Edition, John Wiley, New York, NY, 1975.

[37] M. R. Alexander, S. Payan, T. M. Duc, Interfacial interactions of plasma-polymerized acrylic acid and an oxidized aluminium surface investigated using XPS, FTIR and poly (acrylic acid) as a model compound, Surf. Interface Anal. 26 (1998) 961-973.

[38] T.J. Lee, C.W. Chang, S.G. Hahm, K. Kim, S. Park, D.M. Kim, J. Kim, W.S. Kwon, G.S. Liou, M. Ree, Programmable digital memory devices based on nanoscale thin films of a thermally dimensionally stable polyimide, Nanotechnology 20 (2009) 135204

[39] G. Wen, Z. Ren, D. Sun, T. Zhang, L. Liu, S. Yan, Synthesis of Alternating Copolysiloxane with Terthiophene and Perylenediimide Derivative Pendants for Involatile WORM Memory Device, Adv. Funct. Mater. 24 (2014) 3446–3455

Highlight

1.- Simple WORM memories fabricated by irradiating an aluminum electrode with UV-ozone lamp.

2.- These Al/$AlO_x$-UVO/Al memories retain OFF and ON states for at least $10^3$ times using -1V pulse.

3.- Similar WORM memories can be obtained replacing UVO treatment with a thin PVA layer.

4.- Both type of WORM memories show the same conduction mechanisms in ON and OFF states.